

# Scales in nuclear matter: Chiral dynamics with pion nucleon form factors<sup>\*</sup>

N. Kaiser<sup>a</sup>, M. Mühlbauer, and W. Weise

Physik Department, Technische Universität München, D-85747 Garching, Germany

Received: 16 October 2006 / Revised: 23 November 2006

Published online: 16 January 2007 – © Società Italiana di Fisica / Springer-Verlag 2007

Communicated by U.-G. Meißner

**Abstract.** A systematic calculation of nuclear matter is performed which includes the long-range correlations between nucleons arising from one- and two-pion exchange. Three-body effects from  $2\pi$  exchange with excitations of virtual  $\Delta(1232)$ -isobars are also taken into account in our diagrammatic calculation of the energy per particle  $\bar{E}(k_f)$ . In order to eliminate possible high-momentum components from the interactions we introduce at each pion-baryon vertex a form factor of monopole type. The empirical nuclear matter saturation point,  $\rho_0 \simeq 0.16 \text{ fm}^{-3}$ ,  $\bar{E}_0 \simeq -16 \text{ MeV}$ , is well reproduced with a monopole mass of  $\Lambda \simeq 4\pi f_\pi \simeq 1.16 \text{ GeV}$ . As in the recent approach based on the universal low-momentum  $NN$  potential  $V_{\text{low-}k}$ , the inclusion of three-body effects is crucial in order to achieve saturation of nuclear matter. We demonstrate that the dependence of the pion exchange contributions to  $\bar{E}(k_f)$  on the “resolution” scale  $\Lambda$  can be compensated over a wide range of  $\Lambda$  by counterterms with two “running” contact couplings. As a further application we study the in-medium chiral condensate  $\langle \bar{q}q \rangle(\rho)$  beyond the linear density approximation. For  $\rho \leq 1.5\rho_0$  we find small corrections from the derivative  $d\bar{E}(k_f)/dm_\pi$ , which are stable against variations of the monopole regulator mass  $\Lambda$ .

**PACS.** 12.38.Bx Perturbative calculations – 21.65.+f Nuclear matter

## 1 Introduction and summary

In recent years a novel approach to the nuclear matter problem based on effective field theory has emerged. Its key element is a separation of long- and short-distance dynamics and an ordering scheme in powers of small momenta. At nuclear matter saturation density  $\rho_0 \simeq 0.16 \text{ fm}^{-3}$  the Fermi momentum  $k_{f0}$  and the pion mass  $m_\pi$  are comparable scales ( $k_{f0} \simeq 2m_\pi$ ). Therefore pions must be included as explicit degrees of freedom in the description of the nuclear many-body dynamics. The contributions to the energy per particle,  $\bar{E}(k_f)$ , of isospin-symmetric (spin-saturated) nuclear matter as they originate from chiral pion-nucleon dynamics have been computed up to three-loop order in refs. [1,2]. Both calculations are able to reproduce the empirical saturation point by adjusting one single parameter (either a contact coupling  $g_0 + g_1 \simeq 3.23$  [1] or a momentum cut-off  $\Lambda \simeq 0.65 \text{ GeV}$  [2]) related to unresolved short-distance dynamics. The mechanism for saturation in these approaches is mainly a repulsive contribution to the energy per particle generated by Pauli blocking in second order (iter-

ated) one-pion exchange. As outlined in ref. [2] this mechanism becomes particularly transparent by taking the chiral limit  $m_\pi = 0$ . In that case the interaction contributions to the energy per particle are completely summarized by an attractive  $k_f^3$  term and a repulsive  $k_f^4$  term where the parameter-free prediction for the coefficient of the latter is very close to the one extracted from a realistic nuclear matter equation of state.

This chiral approach to nuclear matter has been extended and improved in ref. [3] by including systematically the effects from  $2\pi$  exchange with excitation of virtual  $\Delta(1232)$ -isobars. The physical motivation for such an extension is threefold. First, the spin-isospin-3/2  $\Delta(1232)$ -resonance is the most prominent feature of low-energy  $\pi N$  scattering. Secondly, it is well known that the  $2\pi$  exchange between nucleons with excitation of virtual  $\Delta$ -isobars generates the medium- and long-range components of the isoscalar central  $NN$  attraction [4]. In phenomenological one-boson exchange models this  $\pi N \Delta$  dynamics is often simulated by a scalar “ $\sigma$ ”-meson exchange. Thirdly, the delta-nucleon mass splitting  $M_\Delta - M_N = 293 \text{ MeV}$  is of the same size as the Fermi momentum  $k_{f0} \simeq 2m_\pi$  at nuclear matter saturation density. Therefore pions and  $\Delta$ -isobars should both be treated as explicit degrees of freedom.

<sup>\*</sup> Work supported in part by BMBF and GSI.

<sup>a</sup> e-mail: nkaiser@ph.tum.de

It has been found in ref. [3] that the inclusion of the chiral  $\pi N\Delta$  dynamics significantly improves, *e.g.*, the momentum dependence of the (real) single-particle potential  $U(p, k_f)$  and the isospin properties (as revealed in the density-dependent asymmetry energy  $A(k_f)$  and the neutron matter equation of state  $\bar{E}_n(k_n)$ ). However, there remain some open questions in these perturbative calculations of nuclear matter. The effective short-range terms are adjusted directly to nuclear matter bulk properties and thus seem unrelated to those relevant for free  $NN$  scattering. Also, no deeper justification for a perturbative treatment of nuclear matter (besides of being very successful) could be given.

Important progress in this direction has come recently from the work of Bogner *et al.* [5] based on the universal low-momentum  $NN$  potential  $V_{\text{low-}k}$ . This potential operates by construction only between the low-momentum nucleon states,  $|\vec{p}| \leq 0.4 \text{ GeV}$ , where it is truly determined by elastic  $NN$  scattering data. It has been demonstrated in ref. [5] that, due to the absence of a model-dependent short-range repulsive core in the potential  $V_{\text{low-}k}$ , its second- and higher-order iterations in nuclear matter (*i.e.* the successive terms in the Brueckner ladder-series) turn out to be small. The primary reason for this (unconventional) feature is the Pauli-exclusion principle: with increasing Fermi momentum  $k_f$  Pauli blocking reduces progressively the available low-momentum phase space wherein  $V_{\text{low-}k}$  acts. Under such conditions a perturbative treatment of the two-body interaction in nuclear matter turns out to be justified. It has also been demonstrated in ref. [5] that a saturation of nuclear matter cannot be achieved from the (low-momentum) two-body interaction alone (see also ref. [6] for earlier Hartree-Fock calculations with  $V_{\text{low-}k}$  exhibiting the same feature). Repulsive three-nucleon interactions (in particular, the long-range ones induced by  $2\pi$  exchange) are crucial in order to stabilize the nuclear many-body system against collapse. As emphasized in ref. [5] in an effective low-energy theory (with a “spatial resolution” of  $\lambda = (0.4 \text{ GeV})^{-1} \simeq 0.5 \text{ fm}$  as it is inherent to the  $V_{\text{low-}k}$  potential) many-body forces are inevitable. Taking into account furthermore the dominant second-order contributions from  $V_{\text{low-}k}$  and the three-nucleon force (adjusted partly to triton and  $^4\text{He}$  binding energies) a saturation minimum of  $\bar{E}_0 \simeq -12 \text{ MeV}$  at the correct equilibrium density  $k_{f0} \simeq 1.35 \text{ fm}^{-1}$  has been obtained. These values correspond to the presently achieved optimum. The theoretical error bar induced by the cutoff variation is discussed in ref. [5] (see fig. 6 therein).

The purpose of the present paper is to reanalyze the chiral approach to nuclear matter from this new perspective and to establish (at least some qualitative) connections to the  $V_{\text{low-}k}$  approach (which actually starts from phase-shift equivalent  $NN$  potentials). As already mentioned, the second-order tensor force from iterated one-pion exchange plays an essential role in order to obtain binding and saturation of nuclear matter in the (perturbative) chiral approaches studied so far [1–3]. On the other hand, its strong short-distance components are one of the sources which render the Brueckner ladder series in nu-

clear matter non-perturbative (*i.e.*, not convergent) [5]. It is therefore advisable to eliminate the high-momentum components from the pion-induced  $NN$  interactions. For that purpose, we follow the phenomenology of the one-boson exchange potentials and introduce at each pion-nucleon interaction vertex a “form factor” of monopole type:

$$F(q^2) = \frac{\Lambda^2 - m_\pi^2}{\Lambda^2 - q^2}, \quad (1)$$

with  $\Lambda$  the monopole mass<sup>1</sup>. Here,  $q^2 \leq 0$  denotes the squared four-momentum transfer carried by the virtual pion. Typical values of the monopole mass  $\Lambda$  employed in one-boson exchange potentials lie in the range  $1.0 \text{ GeV} < \Lambda < 1.7 \text{ GeV}$  [7, 8]. With the form factor  $F(q^2)$  included as a regulator on high-momentum components the  $1\pi$  and  $2\pi$  exchange contributions to the energy per particle  $\bar{E}(k_f)$  depend on the monopole mass  $\Lambda$ . As a first orientation we find that the “natural choice”  $\Lambda \simeq 4\pi f_\pi \simeq 1.16 \text{ GeV}$  (the chiral symmetry breaking scale) reproduces correctly the empirical nuclear matter saturation point:  $\rho_0 = 2k_{f0}^3/3\pi^2 \simeq 0.16 \text{ fm}^{-3}$ ,  $\bar{E}(k_{f0}) \simeq -16 \text{ MeV}$ . As in the  $V_{\text{low-}k}$  approach of ref. [5] the inclusion of the pion-induced three-body terms (with and without virtual  $\Delta$ -isobar excitation) is essential in order to achieve saturation of nuclear matter.

However, a physical low-energy quantity such as the nuclear matter equation of state  $\bar{E}(k_f)$  should not depend on a parameter  $\Lambda$  which merely scans the “spatial resolution” of the pion-baryon interactions involved. We demonstrate that this (unphysical)  $\Lambda$ -dependence of the pion-exchange contributions is, over a large range of monopole masses and densities, almost perfectly counterbalanced by the  $k_f^3$  and  $k_f^5$  terms related to two “running” short-distance contact couplings  $B_{3,5}(\Lambda)$ .

Having reached a description of nuclear matter in terms of explicit pion-exchange dynamics, which is stable against variations of the short-distance scale  $\Lambda$ , we can study the in-medium chiral condensate  $\langle \bar{q}q \rangle(\rho)$  beyond the linear density approximation. These corrections are obtained by differentiating the calculated energy density of nuclear matter  $\rho \bar{E}(k_f)$  with respect to the pion mass (or equivalently, the light quark mass  $m_q$ ). Below the saturation density  $\rho \leq 0.16 \text{ fm}^{-3}$  we find very small corrections. At higher densities a tendency counteracting chiral restoration sets in. Moreover, there is little dependence of the derivative  $d\bar{E}(k_f)/dm_\pi$  on the monopole mass  $\Lambda$  (assuming the short-distance contact couplings  $B_{3,5}(\Lambda)$  to be independent of the quark mass).

Our paper is organized as follows: In sect. 2 we present first the analytical expressions for the one- and two-pion exchange contributions to the energy per particle  $\bar{E}(k_f)$  including the monopole form factors. Then, we discuss in sect. 3 the results for the nuclear matter equation of state together with the compensating short-distance contact couplings  $B_{3,5}(\Lambda)$ . Section 4 is devoted to the in-

<sup>1</sup> The choice of a monopole form factor is primarily for practical convenience.

medium chiral quark condensate  $\langle \bar{q}q \rangle(\rho)$ . Section 5 ends finally with some concluding remarks and an outlook.

## 2 Diagrammatic calculation of the energy per particle

The first contribution to the energy per particle  $\bar{E}(k_f)$  is the kinetic energy of the relativistic Fermi gas of nucleons (expanded in powers of  $1/M_N$ ):

$$\bar{E}(k_f)^{(\text{kin})} = \frac{3k_f^2}{10M_N} - \frac{3k_f^4}{56M_N^3} + \frac{k_f^6}{48M_N^5}. \quad (2)$$

Here,  $k_f$  denotes the Fermi momentum, related to the nucleon density in the usual way,  $\rho = 2k_f^3/3\pi^2$ , and  $M_N = 939$  MeV stands for the (average) nucleon mass. At the densities of interest,  $\rho \leq 0.5 \text{ fm}^{-3}$ , the last term in eq. (2) is already negligibly small ( $< 0.1$  MeV). Next, we enumerate the interaction contributions from one- and two-pion exchange. For each diagram we present only the final result omitting all technical details related to combinatoric and spin-isospin factors and solving the loop and Fermi sphere integrals in the presence of the monopole form factors. Some useful “master integrals” can be found in appendix A of ref. [9].

### 2.1 One-pion exchange Fock term

The contribution of the left  $1\pi$  exchange Fock diagram in fig. 1 (including the relativistic  $1/M_N^2$ -correction) reads:

$$\begin{aligned} \bar{E}(k_f)^{(1\pi)} = & \frac{3g_A^2 m_\pi^3}{(4\pi f_\pi)^2} \left\{ \frac{r^4 - 3r^2 + 2}{8r^4 u} + \arctan(2u) \right. \\ & + \frac{1 - 3r^2}{2r^3} \arctan(2ru) - \frac{1 + 12u^2}{32u^3} \ln(1 + 4u^2) \\ & + \frac{3r^2 - 2 + 12r^2 u^2 (2r^2 - 1)}{32r^6 u^3} \ln(1 + 4r^2 u^2) \\ & + \frac{m_\pi^2}{40M_N^2} \left[ \frac{r^6 - 4r^2 + 3}{2r^6 u} + \frac{3u}{r^4} (3r^4 - 7r^2 + 4) \right. \\ & - (5 + 12u^2) \arctan(2u) \\ & + \frac{1}{2r^5} (25r^2 - 15 - 12r^2 u^2 + 36r^4 u^2) \arctan(2ru) \\ & \left. - \frac{1}{8u^3} \ln(1 + 4u^2) + \frac{4r^2 - 3}{8r^8 u^3} \ln(1 + 4r^2 u^2) \right\}. \quad (3) \end{aligned}$$

For notational simplicity we have introduced the dimensionless variable  $u = k_f/m_\pi$  and the ratio  $r = m_\pi/\Lambda$ . The other occurring parameters are:  $g_A = 1.3$  (the nucleon

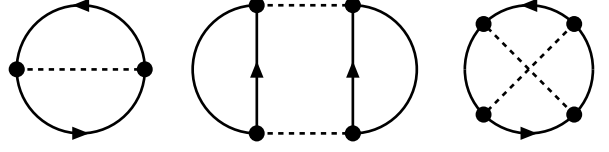


**Fig. 1.** Two-loop one-pion exchange Fock diagram and three-loop iterated one-pion exchange Hartree and Fock diagrams. The combinatoric factors are  $1/2$ ,  $1/4$  and  $1/4$ , in the order shown. Their isospin factors for symmetric nuclear matter are 6, 12 and  $-6$ , respectively.

axial-vector coupling constant),  $m_\pi = 135$  MeV (the neutral pion mass), and  $f_\pi = 92.4$  MeV (the weak pion-decay constant). In the limit  $r \rightarrow 0$  one recovers the result eq. (6) in ref. [2] without the monopole form factor.

### 2.2 Iterated one-pion exchange

The Hartree diagram of the iterated  $1\pi$  exchange (middle diagram in fig. 1) with two medium insertions<sup>2</sup> leads to the following analytical expression:

$$\begin{aligned} \bar{E}(k_f)^{(\text{H}2)} = & \frac{3g_A^4 M_N m_\pi^4}{5(8\pi)^3 f_\pi^4} \left\{ \frac{20(3 + r^2) + 32(1 + r^2)u^2}{1 - r^2} [\arctan(2u) \right. \\ & - \arctan(2ru)] + \frac{1}{u} \left( \frac{1}{2} + \frac{5}{16r^5} - \frac{11}{8r^3} + \frac{41}{16r} + \frac{4}{1+r} \right) \\ & + u \left( 29 - \frac{15}{8r^3} + \frac{41}{4r} - \frac{75r}{8} - \frac{88}{1+r} \right) \\ & + \frac{r^2 - 9 - 20(7 + r^2)u^2}{8(1 - r^2)u^3} \ln(1 + 4u^2) \\ & + \frac{27r^2 - 5 - 63r^4 + 105r^6 + 20r^2 u^2 (1 - 7r^2 + 35r^4 + 35r^6)}{64r^7 (1 - r^2)u^3} \\ & \left. \times \ln(1 + 4r^2 u^2) \right\}. \quad (4) \end{aligned}$$

The corresponding exchange term comes from the Fock diagram of the iterated  $1\pi$  exchange (right diagram in fig. 1) with two medium insertions. While the loop integral including the two squared monopole form factors can be solved there remains a single non-elementary integral from

<sup>2</sup> Medium insertion is the technical notation for the difference between the nucleon propagator in the medium and in the vacuum (see sect. 2 in ref. [2]). To each medium insertion belongs an integration over a Fermi sphere of radius  $k_f$ .

the integration over the Fermi spheres. We get

$$\begin{aligned} \bar{E}(k_f)^{(F2)} &= \frac{3g_A^4 M_N m_\pi^4}{(4\pi u)^3 f_\pi^4} \int_0^u dx x(u-x)^2(2u+x) \\ &\times \left\{ \frac{1+8x^2+8x^4}{2+4x^2} \arctan x - \frac{(1-r^2)^2(1+4x^2)}{(2+4x^2)(1+r^2+4r^2x^2)^2} \right. \\ &+ \left[ 1+2x^2 - \frac{1+r^4+4r^4x^2}{(1+r^2+4r^2x^2)^2} \right] \\ &\times \left[ \arctan \frac{4r^2x}{1-r^2+4r^2x^2} - \arctan \frac{2rx}{1+r} - \arctan \frac{2rx}{1-r} \right] \\ &+ \left[ 1+2x^2 - \frac{1+r^4+4r^4x^2(1+r^2+2r^4x^2)}{4r^2(1+2r^2x^2)^3} \right] \arctan(rx) \\ &+ \left[ \frac{1+r^4+4r^4x^2(1+r^2+2r^4x^2)}{4r^2(1+2r^2x^2)^3} \right. \\ &\left. - \frac{1+r^4+4r^4x^2}{(1+r^2+4r^2x^2)^2} \right] \arctan(2rx) \\ &+ x(1-r^2) \left[ \frac{1+r^{-1}}{1+r^2+4r^2x^2} + \frac{(1-r)^2+4r^2x^2}{(1+r^2+4r^2x^2)^2-4r^2} \right. \\ &\left. + \frac{4rx^2(r^2-2)+5r-9r^{-1}}{16(1+r^2x^2)^2} - \frac{r^{-1}+rx^2(1+r^2)}{(1+2r^2x^2)^2} \right] \Big\}. \quad (5) \end{aligned}$$

In our way of organizing the many-body calculation, the Pauli-blocking effects are represented by diagrams with three medium insertions [2,3]. The contribution of the Hartree diagram with three medium insertions (including the fourth power of a monopole form factor) reads

$$\begin{aligned} \bar{E}(k_f)^{(H3)} &= \frac{9g_A^4 M_N m_\pi^4}{(4\pi f_\pi)^4 u^3} \int_0^u dx x^2 \int_{-1}^1 dy \\ &\times \left[ 2uxy + (u^2 - x^2y^2) \ln \frac{u+xy}{u-xy} \right] \\ &\times \left\{ \frac{2+2r^2}{1-r^2} [\ln(1+r^2s^2) - \ln(1+s^2)] \right. \\ &+ \frac{2s^2+s^4}{1+s^2} + \frac{r^2s^2}{3(1+r^2s^2)^3} [6-6s^2+15r^2s^2 \\ &\left. - 8r^2s^4+7r^4s^4+r^6s^4-3r^4s^6] \right\}, \quad (6) \end{aligned}$$

with the abbreviation  $s = xy + \sqrt{u^2 - x^2 + x^2y^2}$ . On the other hand, one gets from the right Fock diagram in fig. 1 with three medium insertions (including two squared monopole form factors)

$$\begin{aligned} \bar{E}(k_f)^{(F3)} &= \frac{9g_A^4 M_N m_\pi^4}{(4\pi f_\pi)^4 u^3} \int_0^u dx \left\{ \frac{G^2}{8} - \frac{x^2}{4} \int_{-1}^1 dy \right. \\ &\times \int_{-1}^1 dz \frac{yz \theta(y^2+z^2-1)}{|yz| \sqrt{y^2+z^2-1}} \left[ \frac{(1-r^2)s^2}{1+r^2s^2} - \ln(1+s^2) \right. \\ &\left. \left. + \ln(1+r^2s^2) \right] \left[ \frac{(1-r^2)t^2}{1+r^2t^2} - \ln(1+t^2) + \ln(1+r^2t^2) \right] \right\}, \quad (7) \end{aligned}$$

with another abbreviation  $t = xz + \sqrt{u^2 - x^2 + x^2z^2}$  and the auxiliary function

$$\begin{aligned} G &= \frac{u}{r^2}(1-r^2) - \frac{1}{4x}[1+(u+x)^2][1+(u-x)^2] \\ &\times \ln \frac{1+(u+x)^2}{1+(u-x)^2} + \frac{1}{4x}[2r^{-2} - r^{-4} + (u^2 - x^2)^2 \\ &+ 2u^2 + 2x^2] \ln \frac{1+r^2(u+x)^2}{1+r^2(u-x)^2}. \quad (8) \end{aligned}$$

Note that the contributions in eqs. (4)–(7) carry the large-scale enhancement factor  $M_N$ . It stems from the energy denominator of these iterated diagrams which is proportional to the difference of small nucleon kinetic energies.

### 2.3 Irreducible two-pion exchange: spectral representation

Next, we come to the irreducible  $2\pi$  exchange contributions (with no, single, and double  $\Delta(1232)$ -isobar excitation). Their direct evaluation requires the one-loop  $NN$  scattering  $T$ -matrix with a monopole form factor attached to each pion-baryon vertex. The essential long-distance information about these  $2\pi$  exchange one-loop diagrams is already contained in the spectral functions (or imaginary parts). The effect of the monopole form factors<sup>3</sup> on the spectral functions can be easily inferred from the following partial fraction decomposition:

$$\frac{1}{m_\pi^2 - q^2} \left( \frac{\Lambda^2 - m_\pi^2}{\Lambda^2 - q^2} \right)^2 = \frac{1}{m_\pi^2 - q^2} - \frac{1}{\Lambda^2 - q^2} - \frac{\Lambda^2 - m_\pi^2}{(\Lambda^2 - q^2)^2}. \quad (9)$$

It instructs us that a pion exchange with monopole form factors attached to the vertices is identical to a point-like pion exchange minus additional exchanges involving a “heavy particle” of mass  $\Lambda$ . By unitarity this implies that the spectral function of a one-loop  $2\pi$  exchange diagram with monopole form factors has thresholds at  $\mu = 2m_\pi$ ,  $\mu = \Lambda + m_\pi$  and  $\mu = 2\Lambda$ . At the higher thresholds the effective chiral Lagrangian is, however, no more applicable. In this case a meaningful and physically reasonable way to include effects from the monopole form factor is to cut off the spectral integral at  $\mu = \Lambda + m_\pi$ . Putting all pieces together [3] this procedure leads to the following  $2\pi$  exchange two-body Fock term:

$$\begin{aligned} \bar{E}(k_f)^{(2\pi)} &= \frac{1}{8\pi^3} \int_{2m_\pi}^{\Lambda+m_\pi} d\mu \text{Im}(V_C + 3W_C + 2\mu^2 V_T \\ &+ 6\mu^2 W_T) \left\{ 3\mu k_f - \frac{4k_f^3}{3\mu} + \frac{8k_f^5}{5\mu^3} - \frac{\mu^3}{2k_f} - 4\mu^2 \arctan \frac{2k_f}{\mu} \right. \\ &\left. + \frac{\mu^3}{8k_f^3} (12k_f^2 + \mu^2) \ln \left( 1 + \frac{4k_f^2}{\mu^2} \right) \right\}, \quad (10) \end{aligned}$$

where  $\text{Im} V_C$ ,  $\text{Im} W_C$ ,  $\text{Im} V_T$  and  $\text{Im} W_T$  are the spectral functions of the isoscalar and isovector central and tensor

<sup>3</sup> We choose the same monopole form factor for each pion-baryon vertex.

$NN$  amplitudes, respectively. Explicit expressions of these imaginary parts for the contributions of the triangle diagram with single  $\Delta$  excitation and the box diagrams with single and double  $\Delta$  excitation can be easily constructed from the analytical formulas given in sect. 3 of ref. [4]. Note that the  $\mu$ - and  $k_f$ -dependent weighting function in eq. (10) involves two subtractions. This way it is guaranteed that the spectral integral at low and moderate densities is dominated by low invariant  $\pi\pi$  masses,  $2m_\pi < \mu < 1$  GeV. We note also that the method of spectral function regularization has been introduced and studied in detail for elastic  $NN$  scattering by Epelbaum *et al.* [10].

The contributions to the energy per particle from the irreducible  $2\pi$  exchange (with only nucleon intermediate states) can also be cast into the form eq. (10). The corresponding non-vanishing spectral functions read

$$\text{Im } W_C = \frac{\sqrt{\mu^2 - 4m_\pi^2}}{3\pi\mu(4f_\pi)^4} \left[ 4m_\pi^2(1 + 4g_A^2 - 5g_A^4) + \mu^2(23g_A^4 - 10g_A^2 - 1) + \frac{48g_A^4 m_\pi^4}{\mu^2 - 4m_\pi^2} \right], \quad (11)$$

$$\text{Im } V_T = -\frac{6g_A^4 \sqrt{\mu^2 - 4m_\pi^2}}{\pi\mu(4f_\pi)^4}. \quad (12)$$

#### 2.4 Three-body terms with intermediate $\Delta(1232)$ -isobars

Finally, we come to the additional three-body terms which arise from Pauli-blocking of intermediate nucleon states. The corresponding closed Hartree and Fock  $2\pi$  exchange diagrams with single virtual  $\Delta$ -isobar excitation are shown in fig. 2. Their isospin factors are 8, 0 and 8, in the order shown. For the (left) three-loop Hartree diagram the integral over the product of three Fermi spheres of radius  $k_f$  can be solved in the presence of the monopole form factors and its contribution to the energy per particle reads

$$\begin{aligned} \bar{E}(k_f)^{(\text{H3},\Delta)} &= \frac{g_A^4 m_\pi^6}{(M_\Delta - M_N)(2\pi f_\pi)^4} \left\{ \frac{1 + 9u^2 + 3r^2 u^2}{4(1 - r^2)} \right. \\ &\times \left[ \ln(1 + 4r^2 u^2) - \ln(1 + 4u^2) \right] + \frac{4r^2 u^2 + u^4(2r^2 - 1 + 15r^4)}{4r^2(1 + 4r^2 u^2)} \\ &+ \frac{(5 + 3r^2)u^3}{1 - r^2} \arctan(2u) \\ &\left. + \frac{(1 - 15r^2 - 45r^4 - 5r^6)u^3}{8r^3(1 - r^2)} \arctan(2ru) \right\}, \quad (13) \end{aligned}$$

with  $u = k_f/m_\pi$  and  $r = m_\pi/\Lambda$ . The non-relativistic  $\Delta$ -propagator shows up in this expression merely via the (reciprocal) mass splitting  $M_\Delta - M_N = 293$  MeV. Furthermore, we have inserted in eq. (13) already the empirically well-satisfied relation  $g_{\pi N\Delta} = 3g_{\pi N}/\sqrt{2}$  together with the Goldberger-Treiman relation  $g_{\pi N} = g_A M_N/f_\pi = 13.2$ . Finally, the contribution of the right three-body Fock diagram in fig. 2, with two squared monopole form factors included, is given by

$$\bar{E}(k_f)^{(\text{F3},\Delta)} = -\frac{3g_A^4 m_\pi^6 u^{-3}}{4(M_\Delta - M_N)(4\pi f_\pi)^4} \int_0^u dx (2G_S^2 + G_T^2), \quad (14)$$

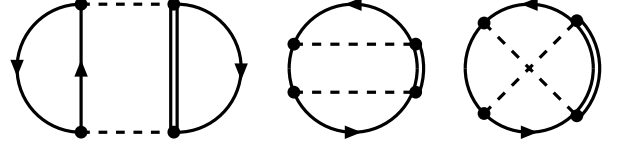


**Fig. 2.** Hartree and Fock three-body diagrams related to  $2\pi$  exchange with single virtual  $\Delta$ -isobar excitation. For symmetric nuclear matter the isospin factors are 8, 0 and 8, in the order shown. The combinatoric factor is 1 for each diagram.

where we have introduced the two auxiliary functions

$$\begin{aligned} G_S &= 4x[\arctan(u+x) + \arctan(u-x)] \\ &+ (x^2 - u^2 - 1) \ln \frac{1 + (u+x)^2}{1 + (u-x)^2} \\ &+ \frac{2x}{r^3} (1 - 3r^2) \{ \arctan[r(u+x)] + \arctan[r(u-x)] \} \\ &+ (u^2 - x^2 + 2r^{-2} - r^{-4}) \ln \frac{1 + r^2(u+x)^2}{1 + r^2(u-x)^2}, \quad (15) \\ G_T &= \frac{1 + u^2 - x^2}{8x^2} [1 + (u+x)^2][1 + (u-x)^2] \\ &\times \ln \frac{1 + (u+x)^2}{1 + (u-x)^2} + \frac{(1 - r^2)u}{2r^4 x} [r^2(1 - u^2 + x^2) - 2] \\ &+ \frac{1}{8} \left[ x^4 + (1 - 3u^2)x^2 + 2u^2 + 3u^4 + r^{-4} \right. \\ &- 2r^{-2} - \frac{u^4}{x^2}(3 + u^2) + \frac{3u^2}{r^4 x^2}(1 - 2r^2) \\ &\left. + \frac{2 - 3r^2}{r^6 x^2} \right] \ln \frac{1 + r^2(u+x)^2}{1 + r^2(u-x)^2}. \quad (16) \end{aligned}$$

Evidently, the three-body Fock term in eq. (14) is attractive and reduces, by about 1/3, the stronger repulsive Hartree term in eq. (13).

### 3 Results for the nuclear matter equation of state

We are now in the position to present numerical results for the nuclear matter equation of state. The interaction contributions to the energy per particle  $\bar{E}(k_f)$  written down in sect. 2 depend on a free parameter, the monopole mass  $\Lambda$ . A first possible option is to adjust it to (one coordinate of) the empirical saturation point. Imposing a minimum of the saturation curve  $\bar{E}(k_f)$  at  $k_{f0} = 262$  MeV (corresponding to an equilibrium density of  $\rho_0 = 0.158$  fm $^{-3}$ ) fixes the monopole mass to  $\Lambda_0 = 1.145$  GeV. This value is surprisingly close to the chiral symmetry breaking scale  $\Lambda_\chi = 4\pi f_\pi \simeq 1.16$  GeV. It is also compatible with the typical monopole masses employed in one-boson exchange potentials [7]. With that fixed  $\Lambda_0$ -value the energy per particle at the saturation minimum comes out as  $\bar{E}_0 = -16.7$  MeV, in good agreement with the empirical value  $\bar{E}_0 = (-16 \pm 1)$  MeV. This is quite a non-trivial result.

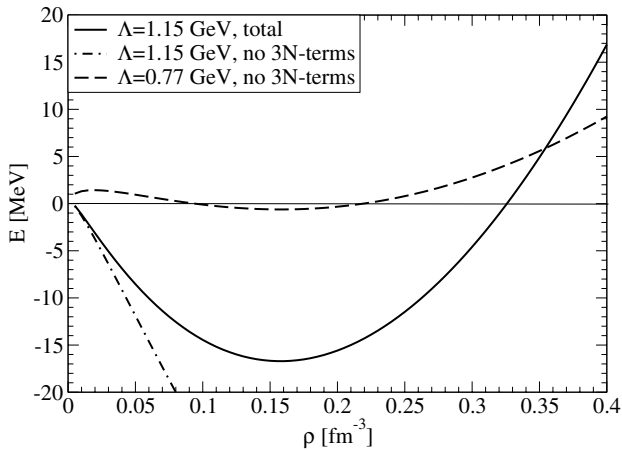


**Fig. 3.** Energy per particle  $\bar{E}(k_f)$  of isospin-symmetric nuclear matter *versus* the nucleon density  $\rho = 2k_f^3/3\pi^2$ . In the dashed lines all three-body terms have been omitted.

The decomposition of  $\bar{E}_0$  into the contribution from the kinetic energy,  $1\pi$  and  $2\pi$  exchange, as well as two- and three-body terms is also interesting:  $\bar{E}_0 = (21.64 + 13.63 - 72.86 - 6.41 + 19.06 - 1.46 + 4.63 + 7.72 - 2.67)$  MeV, where the nine entries correspond to the terms in eqs. (2)–(7), (10), (13), (14), in that order. The total potential energy per particle  $\bar{E}(k_{f0})^{(\text{pot})} = -38.3$  MeV arises from a balance of attractive and repulsive terms, where the largest of them amounts to about 1.9 times the total result. This represents some improvement in comparison to the situation in refs. [2,3] without the monopole form factors but it leaves the question about the “convergence” of the pion loop expansion for nuclear matter still open. The full line in fig. 3 shows the resulting nuclear matter equation of state as a function of the nucleon density  $\rho = 2k_f^3/3\pi^2$  up to about  $2.5\rho_0 \simeq 0.4 \text{ fm}^{-3}$ . The curvature at its minimum translates into a nuclear matter compressibility of  $K = k_{f0}^2 \bar{E}''(k_{f0}) = 292$  MeV. It is about 10% larger than the recent extrapolation from giant monopole resonances of heavy nuclei, which gave the value  $K = (260 \pm 10)$  MeV [11].

The inclusion of the  $2\pi$  exchange three-body terms eqs. (6), (7), (13), (14) is crucial in order to achieve realistic saturation of nuclear matter in our calculation. This feature is in accordance with the findings in the work of ref. [5] based on the universal low-momentum  $NN$  potential  $V_{\text{low-}k}$ . It is also compatible with the results of sophisticated many-body calculations by the Urbana group [12]. The dashed line in fig. 3 shows the effect of turning off the  $2\pi$  exchange three-body terms eqs. (6), (7), (13), (14) in our calculation. After such a truncation there is almost no trace of nuclear matter saturation left over. In order to keep still a very shallow minimum at  $k_{f0} = 262$  MeV the monopole mass has been reduced to  $\Lambda = 0.77$  GeV. Leaving  $\Lambda_0 = 1.15$  GeV unchanged the curve for  $\bar{E}(k_f)$  without three-body terms would just decrease monotonically for all densities  $0 < \rho < 0.4 \text{ fm}^{-3}$ , reaching the huge negative value  $-78.2$  MeV at its lower end. This behavior is indicated (for low densities  $\rho \leq 0.1 \text{ fm}^{-3}$ ) by the dash-dotted line in fig. 3.

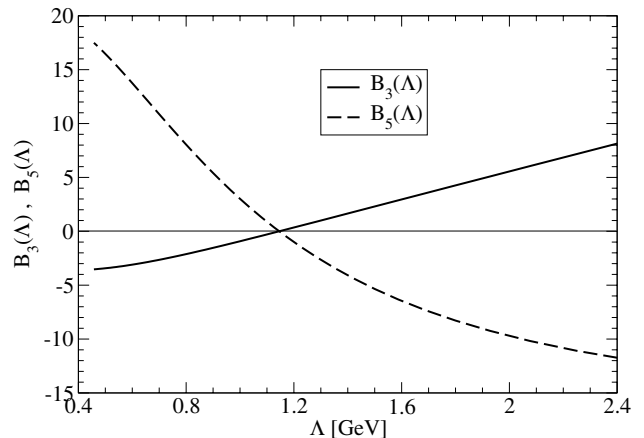


**Fig. 4.** The “running” contact couplings  $B_3(\Lambda)$  and  $B_5(\Lambda)$  as a function of the resolution scale  $\Lambda$ .

The pion-nucleon monopole form factor  $F(q^2)$  introduced in our calculation is only a regulator eliminating high-momentum components. It is not a physical (observable) quantity. Interpreted differently, the monopole mass  $\Lambda$  is a control parameter which monitors the “spatial resolution” at the pion-baryon interaction vertices. A low-energy quantity, such as the nuclear matter equation of state, should not depend on it. We take the point of view, characteristic of an effective field theory, that the explicit pion-exchange terms are accompanied by additional “unresolved” short-distance contributions. The most general  $NN$  contact interaction (momentum-independent and quadratic in momenta) gives rise to the following counterterm contribution to the energy per particle:

$$\bar{E}(k_f)^{(\text{ct})} = B_3(\Lambda) \frac{k_f^3}{M_N^2} + B_5(\Lambda) \frac{k_f^5}{M_N^4}, \quad (17)$$

with  $B_3(\Lambda)$  and  $B_5(\Lambda)$  two dimensionless coupling strengths. In the sense of a “renormalization group equation” we allow these contact couplings to run with the resolution scale  $\Lambda$  such that the physical observable, the total energy per particle  $\bar{E}(k_f)$ , is (as closely as possible) independent of  $\Lambda$ .

Figure 4 shows how the two contact couplings  $B_3(\Lambda)$  and  $B_5(\Lambda)$  must vary with the monopole mass  $\Lambda$  if the nuclear matter saturation point is required to stay fixed. The approximate linear rise of  $B_3(\Lambda)$  over the whole range  $0.4 \text{ GeV} < \Lambda < 2.4 \text{ GeV}$  finds its explanation in the fact that for the iterated  $1\pi$  exchange contributions eqs. (3), (5), the monopole form factor serves also as a regulator on a linearly divergent loop integral (scaling as  $1/r \sim \Lambda$ ) which contributes to the energy per particle linear in density ( $\rho \sim k_f^3$ ). In the window  $0.9 \text{ GeV} < \Lambda < 1.5 \text{ GeV}$  of monopole masses the contact couplings can be considered as being of “natural” size:  $|B_{3,5}(\Lambda)| < 6$ .

In fig. 5 we show the resulting nuclear matter equation of state for three different monopole masses  $\Lambda = 0.5$  GeV,  $1.0$  GeV and  $1.5$  GeV. In the density region  $0 < \rho < 0.4 \text{ fm}^{-3}$  there is almost no dependence on the resolution scale  $\Lambda$  left over. As expected, the small spreading of the three curves increases with increasing Fermi

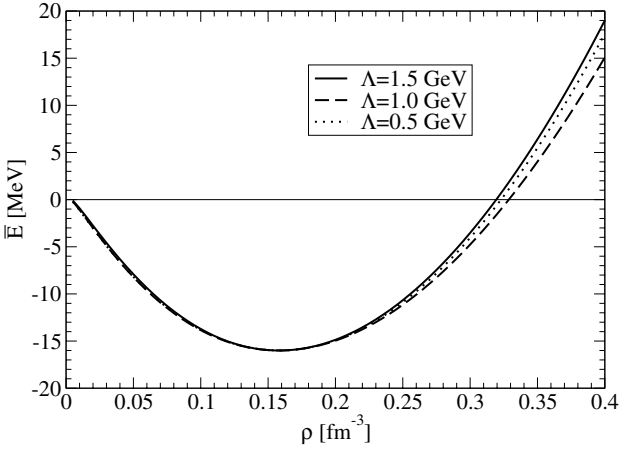


**Fig. 5.** Energy per particle  $\bar{E}(k_f)$  of isospin-symmetric nuclear matter *versus* the nucleon density  $\rho = 2k_f^3/3\pi^2$ . The curves correspond to three different monopole masses  $\Lambda = 0.5$  GeV, 1.0 GeV and 1.5 GeV with the contributions of the compensating contact couplings  $B_{3,5}(\Lambda)$  included.

momentum  $k_f$ , where higher-momentum components of the interactions get probed more sensitively. It is also astonishing to observe that the rather complicated density dependence of the  $r$ -dependent terms ( $r = m_\pi/\Lambda$ ) written down in sect. 2 can be almost perfectly counterbalanced by two leading powers of the Fermi momentum,  $k_f^3$  and  $k_f^5$ , reflecting contact interactions without and with two derivatives. We have investigated the differences in the energy per particle with respect to the case  $\Lambda_0 = 1.15$  GeV where the running contact couplings are zero:  $B_3(\Lambda_0) = B_5(\Lambda_0) = 0$ . For a wide range of monopole masses,  $0.4 \text{ GeV} < \Lambda < 2.5 \text{ GeV}$ , these deviations oscillate merely between  $+1.5$  MeV and  $-1.0$  MeV in the whole density region  $0 < \rho < 0.5 \text{ fm}^{-3}$ . Therefore, one can speak of a pretty stable nuclear matter saturation curve in our calculation which combines pion exchange dynamics including a regularizing monopole form factor with (two) scale-dependent short-distance contact couplings. As a supplementary information we give also for  $\Lambda = 0.75$  GeV the contributions to the total potential energy:  $\bar{E}(k_{f0})^{(\text{pot})} = (11.3 - 33.6 - 1.4 + 13.0 - 1.0 + 3.6 + 5.2 - 1.8 - 33.7)$  MeV, where the last entry corresponds to the counterterm in eq. (17). Now each individual contribution is (in magnitude) smaller than 0.9 times the total result.

#### 4 Chiral condensate at finite density

The chiral condensate  $\langle 0|\bar{q}q|0\rangle$  is an order parameter of spontaneous chiral symmetry breaking. With increasing temperature the chiral condensate decreases (or “melts away”). For low temperatures this effect can be systematically calculated in chiral perturbation theory. At three-loop order [13] the estimate  $T_c \simeq 190$  MeV of the critical temperature, where chiral symmetry will be eventually restored, has been found. This (extrapolated) value of  $T_c$  is remarkably consistent with the recent result  $T_c =$

$(192 \pm 8)$  MeV obtained in numerical simulations of full QCD on the lattice [14]. The chiral condensate drops also with increasing baryon density. The leading linear term in the nucleon density  $\rho$  is readily derived (via the Feynman-Hellmann theorem) by differentiating the energy density of a nucleonic Fermi gas,  $\rho M_N + \mathcal{O}(\rho^{5/3})$ , with respect to the light quark mass  $m_q$ . This introduces the nucleon sigma-term  $\sigma_N = \langle N|m_q\bar{q}q|N\rangle = m_q \partial M_N / \partial m_q$  as the driving term for the density evolution of the chiral condensate. Corrections beyond the linear density approximation arise from the  $NN$  interactions which transform the nucleonic Fermi gas into a nuclear Fermi liquid. Because of the Goldstone boson nature of the pions,  $m_\pi^2 \sim m_q$ , the explicit pion exchange dynamics in nuclear matter plays a particularly important role for the in-medium chiral condensate  $\langle \bar{q}q\rangle(\rho)$ . Converting quark mass derivatives into pion mass derivatives and using the Gell-Mann-Oakes-Renner relation  $m_\pi^2 f_\pi^2 = -m_q \langle 0|\bar{q}q|0\rangle$  one finds for the ratio of the in-medium to vacuum chiral condensate

$$\frac{\langle \bar{q}q\rangle(\rho)}{\langle 0|\bar{q}q|0\rangle} = 1 - \frac{\rho}{2m_\pi f_\pi^2} \left[ \frac{2\sigma_N}{m_\pi} + \frac{d\bar{E}(k_f)}{dm_\pi} \right]. \quad (18)$$

The nucleon sigma-term

$$\sigma_N = m_q \frac{\partial M_N}{\partial m_q} = \frac{m_\pi}{2} \frac{\partial M_N}{\partial m_\pi} \quad (19)$$

measures that portion of the nucleon mass  $M_N$  which arises from the explicit chiral symmetry breaking in QCD (*i.e.*, the non-vanishing up/down quark mass  $m_q \neq 0$ ). The empirical value of  $\sigma_N$  as extracted from dispersion relation analyses of  $\pi N$  scattering data is  $\sigma_N = (45 \pm 8)$  MeV [15].

From our nuclear matter calculation with explicit one- and two-pion exchange dynamics we can now easily compute the derivative  $d\bar{E}(k_f)/dm_\pi$  of the energy per particle with respect to the pion mass. In addition to the explicit  $m_\pi$ -dependence we consider also the implicit one through the nucleon mass:  $\partial M_N / \partial m_\pi = 2\sigma_N / m_\pi \simeq 0.67$ . The smaller and less well-known quark mass derivatives of the axial-vector coupling constant  $g_A$  and the pion decay constant  $f_\pi$  are neglected at present. For example, the one-loop chiral perturbation theory gives for the pion decay constant the small derivative:  $\partial f_\pi / \partial m_\pi = (\bar{l}_4 - 1)m_\pi / (8\pi^2 f_\pi) \simeq 0.063$  [16]. Furthermore, from the combination of lattice QCD results for  $g_A$  and their chiral extrapolation [17] one estimates  $m_\pi \partial g_A / \partial m_\pi \leq 0.05$  around the physical point. Corrections to  $d\bar{E}(k_f)/dm_\pi$  from the  $m_\pi$ -dependence of the  $\pi N$  coupling constant  $\sim g_A/f_\pi$ , are therefore expected to be small, less than 5%.

Figure 6 shows the dropping chiral condensate  $\langle \bar{q}q\rangle(\rho)$  as a function of the nucleon density up to  $\rho = 0.4 \text{ fm}^{-3}$ . The full line corresponds to the linear density approximation using the central value  $\sigma_N = 45$  MeV. The other curves include the effects of nuclear correlations through the derivative  $d\bar{E}(k_f)/dm_\pi$  for various values of the monopole mass  $\Lambda$ . We have assumed that the short-distance contact couplings,  $B_3(\Lambda)/M_N^2$  and  $B_5(\Lambda)/M_N^4$ , which keep the saturation curve  $\bar{E}(k_f)$  stable (see sect. 3)

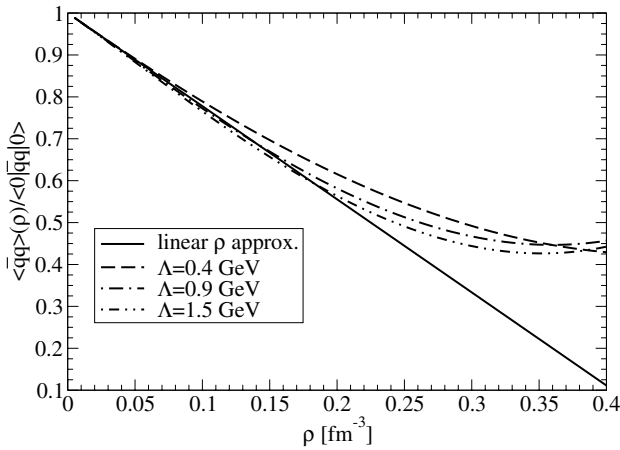


**Fig. 6.** Density dependence of the chiral quark condensate  $\langle \bar{q}q \rangle(\rho)$ .

are quark mass independent. This is a natural assumption, but difficult to substantiate further. If we use the naive dimensional analysis of refs. [18,19] to estimate the quark mass dependence,  $B_3(\Lambda) = B_3^{(0)}(\Lambda) + \alpha_3(m_\pi/\Lambda_\chi)^2$  together with the generous bound  $|\alpha_3| < 5$ , we find at  $\rho_0 = 0.16 \text{ fm}^{-3}$  at most a 1% effect on the condensate ratio eq. (18).

One observes in fig. 6 that up to equilibrium density  $\rho_0$  the corrections beyond the linear density approximation are in fact very small. This finding can be taken as an *a posteriori* justification of the assumption made in ref. [20] about the in-medium behavior of the scalar mean field  $\Sigma_S^{(0)}$ . At higher densities a trend counteracting chiral restoration sets in. Similar features have been observed in the earlier chiral approach of Lutz *et al.* [1] as well as in ref. [21] where the relativistic scalar-vector mean-field phenomenology has been combined with estimates of the quark mass derivatives. It is comforting to see that the explicit one- and two-pion exchange dynamics does not lead to the opposite trend, namely acceleration of chiral restoration, which would undermine the foundation of the present approach to nuclear matter, based on the spontaneous breaking of chiral symmetry (in the vacuum).

Finally, one should note that the nucleon sigma-term  $\sigma_N$  has presently a sizable uncertainty of  $\pm 18\%$ . Therefore, the error band associated with the linear density approximation  $1 - \rho \sigma_N / (m_\pi^2 f_\pi^2)$  masks practically all effects from nuclear correlations at least up to nuclear matter saturation density,  $\rho_0 = 0.16 \text{ fm}^{-3}$ .

## 5 Concluding remarks and outlook

In this work we have performed a nuclear matter calculation which treats the long-range correlations from one- and two-pion exchange explicitly. In accordance with the recent approach of ref. [5] based on the  $V_{\text{low-}k}$  potential we find that repulsive three-body terms are essential in order to achieve realistic binding and saturation of nuclear matter. As a novel feature we have introduced a pion-nucleon

monopole form factor as a regulator to eliminate high-momentum components from the interactions. The dependence on the “resolution” parameter, the monopole mass  $\Lambda$ , can be perfectly counterbalanced by two running short-distance contact couplings  $B_{3,5}(\Lambda)$ . The resulting nuclear matter equation of state  $\bar{E}(k_f)$  is stable against variations of  $\Lambda$ . We have taken the pion mass derivative  $d\bar{E}(k_f)/dm_\pi$  and obtained small corrections to the in-medium chiral condensate  $\langle \bar{q}q \rangle(\rho)$  beyond the linear density approximation.

A more detailed comparison of the present nuclear matter calculation with the one based on the  $V_{\text{low-}k}$  potential [5] offers prospects for a better understanding of the relevant short-range  $NN$  dynamics, which so far enters in the form of two adjusted contact couplings  $B_{3,5}(\Lambda)$ . Work along these lines is in progress [22].

We thank Achim Schwenk for many useful discussions.

## References

1. M. Lutz, B. Friman, C. Appel, Phys. Lett. B **474**, 7 (2000).
2. N. Kaiser, S. Fritsch, W. Weise, Nucl. Phys. A **697**, 255 (2002).
3. S. Fritsch, N. Kaiser, W. Weise, Nucl. Phys. A **750**, 259 (2005) and references therein.
4. N. Kaiser, S. Gerstendörfer, W. Weise, Nucl. Phys. A **637**, 395 (1998).
5. S.K. Bogner, A. Schwenk, R.J. Furnstahl, A. Nogga, Nucl. Phys. A **763**, 59 (2005) and references therein.
6. J. Kuckei, F. Montani, H. Mütter, A. Sedrakian, Nucl. Phys. A **723**, 32 (2003).
7. R. Machleidt, K. Holinde, C. Elster, Phys. Rep. **149**, 1 (1987).
8. R. Machleidt, Phys. Rev. C **63**, 024001 (2001) and references therein.
9. N. Kaiser, S. Fritsch, W. Weise, Nucl. Phys. A **724**, 47 (2003).
10. E. Epelbaum, W. Glöckle, Ulf-G. Meißner, Eur. Phys. J. A **19**, 125 (2004).
11. D. Vretenar, T. Nikšić, P. Ring, Phys. Rev. C **68**, 024310 (2003).
12. A. Akmal, V.R. Pandharipande, D.G. Ravenhall, Phys. Rev. C **58**, 1804 (1998) and references therein.
13. P. Gerber, H. Leutwyler, Nucl. Phys. B **321**, 387 (1989) and references therein.
14. M. Cheng *et al.*, Phys. Rev. D **74**, 054507 (2006).
15. J. Gasser, H. Leutwyler, M.E. Sainio, Phys. Lett. B **253**, 252 (1991).
16. G. Colangelo, J. Gasser, H. Leutwyler, Nucl. Phys. B **603**, 125 (2001).
17. T.R. Hemmert, M. Procura, W. Weise, Phys. Rev. D **68**, 075009 (2003); M. Procura, B.U. Musch, T.R. Hemmert, W. Weise, hep-lat/0610105.
18. E. Epelbaum, Ulf-G. Meißner, W. Glöckle, Nucl. Phys. A **714**, 535 (2003).
19. S.R. Beane, M.J. Savage, Nucl. Phys. A **717**, 91 (2003).
20. P. Finelli, N. Kaiser, D. Vretenar, W. Weise, Nucl. Phys. A **770**, 1 (2006) and references therein.
21. R. Brockmann, W. Weise, Phys. Lett. B **367**, 40 (1996).
22. N. Kaiser, A. Schwenk, W. Weise, in preparation.